9 Conclusions and Further Suggestions

9.1 SkyPlot

The skyplots show immediately that a strategy for observing involving the correct look angle is imperative in some cases. A fixed telescope looking solely in one direction for the duration of its observing run will miss some debris, whereas its detection rate could be optimised by repointing the scope to a nearby "hot spot". Choice of observing site also has an important effect, for example the fourfold difference in total visibility over the year for a Mir-like orbit observed from sites at Siding Springs and Pic Du Midi (chapter 5).

Type of orbit is important too - it appears from analysis of just one type of highly eccentric orbit (Molniya) that visibility varies as a function of topocentric angular speed (ω_{top}). Debris near perigee is far less visible than at other points in its orbit (and therefore at greater range), despite its closer proximity, at least for debris of the size in this study (10cm). Smaller debris would cease to be visible before reaching the heights near apogee of the 10cm debris - an optimum range of true anomaly probably exists where the debris is neither too far away, nor moving too fast, to be detectable.

The above is based on studies of is Molniya orbits only however - it remains to be seen if the same can be said for other highly eccentric orbits of different inclinations: GTO orbits launched from the USA, French Guiana, and Russia, for example.

Look angle is therefore a consideration to undertake seriously for LEO & Molniya orbits at least. It has less of an effect for Iridium and GPS constellations, though this may well be due to the number of orbit planes in those constellations - results from individual orbit planes were summed, thus possibly smearing out any SkyPlot patterns from individual planes.

9.1.1 Further suggestions

Although some speed optimisation techniques were used in the design of the program, execution time is still on the order of several hours for one year-long simulation, for example. Performing an analytical approach to the rise/set times

of debris, i.e. to calculate in advance the times and dates of these events, so that time isn't devoted to incrementing the debris through periods when it is below the horizon and all other visibility conditions are immaterial, would be useful.

It would be interesting to improve on the debris model itself by taking into account the characteristics of certain types of debris known to exist; an analysis of the Na-K reactor RORSAT coolant droplet population would be interesting.

Rather than using event plots ("dot plots") to mark the alt-az positions of visibility flag changes, continuous colour-coded trajectory plots may be better suited to analysis of the causes of the skyplot patterns.

Including periods of twilight and those when the moon is in the sky, improving the latitude capability of the model to incorporate sites up to ±90º, incorporating basic weather conditions for each site and adding light pollution effects and those due to aurora would all extend the capability of the model.

The number of particles used to populate the orbit could be increased, to produce a more continuous flow of particles per orbit. One hundred particles were used in chapter 5 in order to keep run time overheads low on the computing system.

In addition to observatories, skyplots could be made for a global grid of theoretical sites, in time increments of one month or shorter, to produce an "EarthPlot" contour map showing the best sites for observing certain orbits.

9.2 Debris Detection (DDT) Program

Due to the lack of suitable real images to run the DDT program on, the results are for the performance characteristics of the DDT program itself, rather than for results pertaining to debris imagery.

Results show that the DDT program works better for slower and therefore higher debris, i.e. not for LEO. Centimetric debris detection by radar is well underway for objects in LEO however, so where radar sensitivity begins to fall off, this detection program may have some utility. Given a fast readout CCD with low noise characteristics and a wide FOV optical system, debris in high LEO (~1000km) could be detected.

9.2.1 Further suggestions

The DDT program could be improved by changing the manner in which the currently used program delineates its search areas and predicted positions to match the exact shapes described in chapter 7. The current system is an approximation that uses rectangular shapes that errs on the side of computing speed and oversensitivity - i.e. the system would spot all debris but would also cause some erroneous noise-induced tracks to be “detected”. It was thought this solution was preferable to underpredicting and missing some debris, or calculating exact search area bounds and increasing run time, thus missing some of the faster debris.

Rather than calculating such involved shapes for the search area to ensure the debris track does not finish outside the FOV, the initial pair produced from frames 1 and 2 could just be extrapolated ahead by N frames (N = length of moving bracket) to see if it finishes outside the FOV. A test to see if this method would be quicker than calculating the explicit search area shapes could be made.

The rasterscan approach is just one way to interrogate the dots in the frame 2 search area to determine those that could possibly be part of a debris track. Another method suggested by James Dick of the RGO is to utilise the run-length-encoded nature of the output from the front end and use indexing and hash tables as a means of searching those dots within the search area (whose bounds are still calculated following the same technique). A test to observe speed of execution under both methods should be undertaken.

The rasterscan method could be accelerated however by implementing a different numbering regime when writing the input picture files to the virtual frames of the moving bracket. Instead of writing a 1 or 0 to denote the presence of a dot, a number representing the current picture file number could be written instead, and the DDT program instructed to search for that number only, ignoring all others. In this way the used frames in the bracket need not be flushed to make way for new pictures, as they currently are now, thus improving speed.

Finally, an interesting approach would be to include all detection characteristics of the DDT program into the SkyPlot program, i.e. adapting the SNR calculation of the latter to reflect the sensitivity of the former.

9.2.1.1 Asteroid detection with the DDT

Given that the DDT is best suited for picking out slow moving objects from noisy backgrounds, an interesting area of investigation would be to attempt to use it for the detection of asteroids. The timing considerations are less strict; integration times are longer, and readout times could be much longer, safely on the order of many seconds or minutes, well within the capabilities of astronomical equipment today.

The DDT program could operate in three modes: to detect space debris; to detect fast Near-Earth asteroids (NEAs); and to detect the much slower Kuiper Belt objects.

NEAs, as the name suggests, are asteroids whose orbits bring them close to the Earth. They are generally divided into three somewhat arbitrary families: Apollo, Amor and Aten objects. The Apollo and Aten orbits actually cross the Earth's orbit, while Amors have perihelions just outside the Earth's aphelion. Kuiper belt objects are a relatively recent discovery, whose orbits lie beyond that of Neptune, i.e. > ~30AU (Kowal, 1996).

The detection strategy by which the DDT program must operate to detect NEAs depends on the typical range of topocentric angular velocities they would exhibit. Considering a very close flyby of a typical NEA, say at a distance of GSO (~36000km), and at a relative velocity of 20km s^{-1}, the value of ω_{top} is ≈115 arcsec s^{-1}, comparable to a debris orbit of 8-10,000 km. This is well inside the detection limit caused by timing constraints (see section 8.3.2) and so would be achievable by the DDT running on a 350MHz Pentium. Such a flyby would be a rare encounter however – of the 21 closest approaches catalogued so far, only 4 have come within the orbit of the Moon. The closest was by 1994 XM1, which passed by at 0.0007 AU (104,000 km), whereas the mean distance from this sample is 0.0051 AU (760,000 km) (Williams, 1999).

The direction of the asteroid's velocity vector through the FOV would not be known in advance to a great degree, because although its orbital inclination may

be close to the ecliptic, the proximity of a close approach would make the relative position and velocity vectors depart greatly from the plane of the ecliptic.

For these reasons a circular search area around the precursor or "frame 1" centroid in the search algorithm, would be retained, leading to essentially the same setup for observing NEAs as for space debris.

If one does not want to search for NEAs at very close approach, then the angular velocity would be much smaller. In this case any asteroids near the centre of the FOV at the start of the observing run would remain in the FOV for many frames before drifting out of the FOV. For this reason all centroids in frame 1 could be viable precursors to an asteroid track, so the program could start by considering all points in the first frame of the moving bracket, then with each bracket analysis, create and gradually expand a "dead zone" in the centre of the FOV (thus creating an active border), following the likelihood of asteroids having drifted away from the centre of the FOV (Figure 9.1).

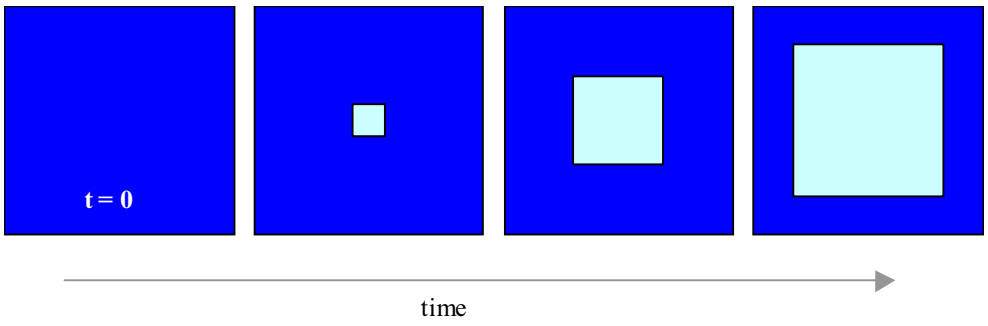

Figure 9.1: Schematic showing the creation of an active border in successive "frame 1" positions in the analysis moving bracket. The dark blue area denotes the part of the frame that is scanned for possible asteroid track precursors, whereas the pale blue region marks the area that is ignored. At the beginning of an observing run therefore, all of the first frame is considered viable.

For Kuiper Belt objects the situation is different in terms of the angular velocities likely to be encountered. Due to the great distance of 30 AU, the angular speed is 3 arcsec hour^{-1} (Rabinowitz, 1991), and the direction of the velocity vector would be constrained to a narrow range of angles centered on the ecliptic. In this case, as the velocity vector in the FOV is well known, the search area may be constrained and take on a different shape to those used for space debris and NEAs, i.e. it could be a small narrow "fan" shape instead (Figure 9.2).

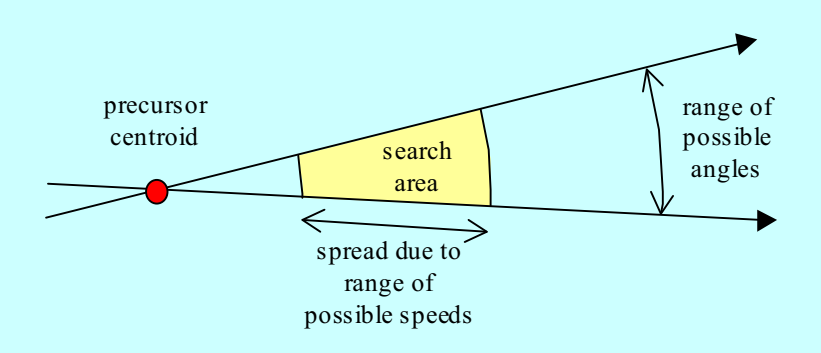

Figure 9.2: Illustration of smaller and narrower search area that would be employed in the search for slow moving asteroids for which the range of probable trajectories was better known.

In this case the angular speed of the asteroids is of the order of 3 arcsec per hour, so asteroids in and near the centre of the FOV would not move far from the centre even during the course of the whole night (~ 10 hours). Also, the time between frames would also be of the order of an hour or more, plus computing overheads are further reduced because of the much smaller search areas (Figure 9.2). Speed is therefore not as important as it is in the case of debris and NEA searches, and for this reason the active border strategy could be dispensed with.

In the event that the search pattern adopted by the observer produces frames taken at irregular intervals for whatever reason, the DDT code could be modified by tagging the time onto each frame; i.e. passing a “timestamp” for each frame through to the DDT program as it runs. As the frame interval for Kuiper Belt objects would be of the order of many minutes to an hour or more, and the angular speed in the image plane would be into the sub-pixel per second range, a timestamp accurate to the nearest second would be adequate, and can be generated easily by either the telescope or DDT software using the computing system clock.

As each new picture is read into the analysis bracket, its timestamp would be read into a separate “timestamp bracket” or array, to be accessed in tandem later using the same cyclic counter pointer driver in the code which is used for the image analysis.

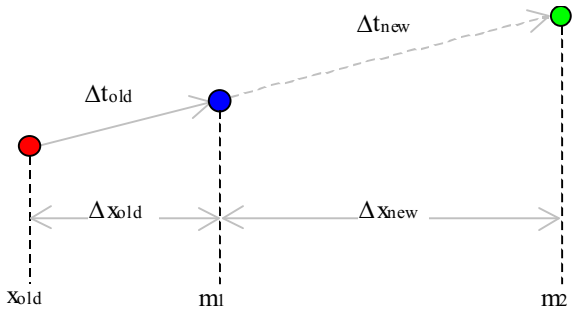

Figure 9.3: Illustration of how predicted positions are calculated with irregular frame intervals. Only the x coordinates are shown for clarity. The red, blue and green dots denote centroids under scrutiny from the previous, current and next frames respectively. See text for details.

With reference to Figure 9.3, when a line of dots is being analysed, the "next" position in line (i.e. the predicted position) would be calculated by multiplying the Δx and Δy values generated from the previous-to-current frames, by the ratio of frame interval calculated from the current-to-next frame interval (Δt_{new}) over that of the previous-to-current frame (Δt_{old}).

In other words:

$$\Delta t_{old} = \text{timestamp } [\textit{CURRENT FRAME}] - \text{timestamp } [\textit{PREVIOUS FRAME}], \quad (9.1)$$

$$\Delta t_{new} = \text{timestamp } [\textit{NEXT FRAME}] - \text{timestamp } [\textit{CURRENT FRAME}], \quad (9.2)$$

and therefore:

$$T_{ratio} = \frac{\Delta t_{new}}{\Delta t_{old}} \ . \quad (9.3)$$

In Figure 9.3 the x coordinate of the centroid being analysed in the current frame is denoted by m_1; that of the previous frame by x_{old}, and that of the next frame, i.e. the centre of the predicted position to be scanned next, is depicted as m_2. This treatment is restricted to x components only, for clarity (the same treatment applies to y components).

The Δx distance from the previous frame to the current frame is given by:

$$\Delta x_{old} = m_1 - x_{old} \ , \quad (9.4)$$

so that the distance from the present to the next predicted position is calculated as:

$$\Delta x_{new} = x_{old} \times T_{ratio} \ . \quad (9.5)$$

Given the amount of time available between frames, the observer could perform the DDT “front end” tasks of thresholding and centroiding etc themselves, using existing Starlink software. The list of centroid positions thus produced would then be fed into the DDT program for analysis as usual, possibly enabling a search program to be modified at the observatory during the night should an object be detected, to obtain accurate photometry, etc.